Journal of the European Ceramic Society **19** (1999) 263–270

PII: S0955-2219(98)00196-4
0955-2219/98/$—see front matter

Low Pressure Lamination of Ceramic Green Tapes by Gluing at Room Temperature

Michael A. Piwonski and Andreas Roosen*

University of Erlangen-Nuremberg, Department of Materials Science, Glass and Ceramics, Martensstr. 5, D-91058 Erlangen, Germany

(Received 28 March 1998; accepted 7 August 1998)

Abstract

An advanced method to laminate ceramic green tapes is described. In contrast to the well-known thermo-compression method, in which a junction is produced at elevated temperatures and pressures, this method allows the laminates to be produced at room temperature under very low pressures. To aid the joining of the tapes, an adhesive system was utilised: a double-sided adhesive tape, consisting of an acrylate adhesive and a carrier film made of polyethyleneterephthalate (PET). The studies were carried out on two alumina-based green tapes having different grain sizes. The laminates were characterised in the sintered state using a scanning electron microscope. The polymeric reactions occurring during heat treatment were revealed by optical microscopy experiments, thermogravimetric analysis (TGA), differential scanning calorimetry (DSC) and viscosity measurements. It was found that for a successful joining, a low viscosity polymer melt is necessary. At elevated temperatures it functions as a flux for the ceramic particles, allowing them to rearrange. Due to capillary actions the flux creates a drag on the ceramic layers, leading to interpenetration and a homogeneous body. © *1998 Elsevier Science Limited. All rights reserved*

Keywords: joining, tape casting, lamination, microstructure-prefiring, Al_2O_3.

1 Introduction

Lamination of green tapes is an important process in the manufacturing of layered ceramic structures. First developed for multilayer capacitors, this technique has become the basis for the production of IC packages, actuators, etc.[1] Furthermore it has become increasingly important for structural applications, such as heat exchangers,[2] functional applications like solid oxide fuel cells (SOFC)[3] and for rapid prototyping by lamination.[4]

The basic method used for lamination is the thermo-compression method, in which the different layers are stacked and pressed at temperatures above the binder's glass transition point. The literature is inconsistent with regard to the lamination conditions. Mistler *et al.*[5] gives lamination temperatures of 25–110°C with pressures between 1·38 and 138 MPa. Reed[6] narrows down these ranges to lamination temperatures of 50–80°C with pressures between 3 and 30 MPa. The drawback of the thermo-compression method is that it is difficult to produce fine, undercut, three-dimensional structures. Due to the inhomogeneous pressure distribution around cavities, delamination as well as welding can take place.[6]

According to Hellebrand,[7] for a good homogeneous junction of the green tapes it is crucial to ensure good interpenetration of the powder particles. He also points out the importance of the ratio of binder, powder and pores in the green tape for the thermo-compression process. If the optimum ratio is not used, the particles cannot sufficiently move under the applied pressure. Under optimum conditions, the particles can glide facilitating the tapes to interpenetrate each other, leading to a defect-free homogeneous body. This is illustrated in Fig. 1.

The application of high pressures and temperatures opposes the goal of producing exact, fine-structured and complex laminated structures. Therefore completely new ways of joining green tapes which circumvent the drawbacks of the thermo-compression method are of high interest. The main task is to reduce the lamination pressure and temperature as much as possible. A way to realise this is to utilise gluing techniques for the lamination procedure.

*To whom correspondence should be addressed.

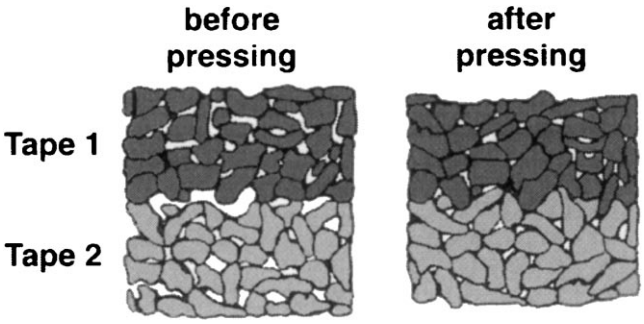

Fig. 1. Arrangement of the particles before and after the lamination process according to Hellebrands model.[7]

2 Experimental Procedure

The lamination experiments were carried out on two different alumina-based green tapes. They were made using the doctor blade method on a laboratory tape-casting machine.

An organic binder system on the basis of polyvinyl butyral (PVB) with dibutylphthalate (DBP) as a plastiziser in a methyl-ethyl-ketone (MEK)/ethanol solution was used for both tapes.[8,9] The batch was the same for both tapes with the exception of the ceramic powder. In the first case the powder was an Alcoa A16 SG with a mean particle size of 0·5 μm, 0·5 mass% MgO was added as a grain growth inhibitor. This tape is denoted as Tape A. The other tape, referred to as Tape B, consists of 96 mass% Alcoa CL2500 SG with a mean particle size of 3·1 μm, with the remaining 4 mass% being ball-milled soda-lime-silica glass.

Using a moving carrier tape velocity of 23·4 cm min^{-1}, 500–700 μm thick green tapes were produced. For the lamination experiments, the tapes were cut into square pieces having a length of 30 mm. As a vehicle for the lamination process a double-sided adhesive tape was applied to the green tapes. A schematic of the structure is shown in Fig. 2.

The adhesive (2 and 6) consists of a polyacrylate. The intermediate backing (4) is made of polyethyleneterephthalate (PET), commonly denoted as polyester. It functions as a carrier for the adhesive. The PET film is approximately 12 μm thick, the total thickness amounting to 48 μm.

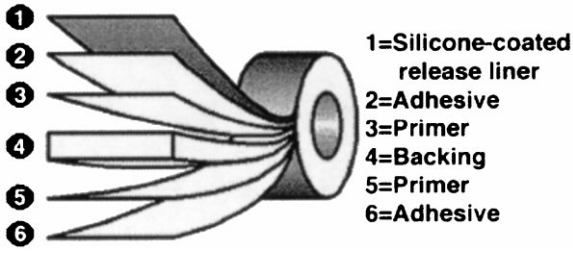

Fig. 2. Structure of the double-sided adhesive tape (© 1998 Elsevier Science Limited. All rights reservedBeiersdorf AG, Hamburg, Germany).[10]

Laminates were made of each of the green tape types using the adhesive tape. Each laminate consisted of 3 layers. The lamination process is illustrated in Fig. 3. In the first step, the gluing material was applied to the green tapes. The double-sided adhesive tape strips were rolled onto the samples with a soft rubber roll, then the release liner was removed. In the second step, the pieces were stacked at room temperature and pressed at 2·5 or 5 MPa. In the last step, binder burn-out and sintering of the specimens were performed using a careful firing scheme, shown in Fig. 4. Low heating rates were chosen to avoid any damages to the specimens due to excessive gas development.

Polished cross sections of the laminates were analysed using a scanning electron microscope. To characterise the joining mechanism, all organic materials were analysed by thermogravimetric analysis (TGA), differential scanning calorimetry (DSC) and dynamic viscosity measurements. All measurements were performed at a heating rate of 1 K min^{-1}. The TGA experiments were carried out in a 951 Thermogravimetric Analyzer from DuPont Instruments. The measuring unit for the DSC experiments was a DuPont Instruments 910 base unit and a 920 Auto-DSC. Furthermore, the pure binder system, consisting of the binder and the plasticizer, as well as the PET of the double-sided adhesive tape were submitted to dynamic viscosity measurements. A CSM 50 from Bohlin

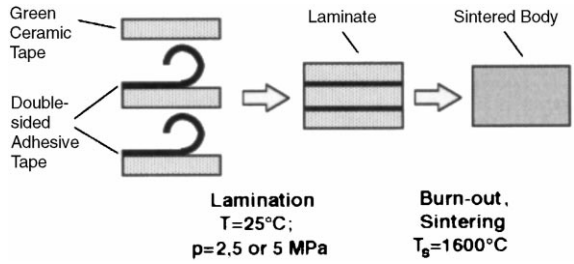

Fig. 3. Processing steps in the new process.

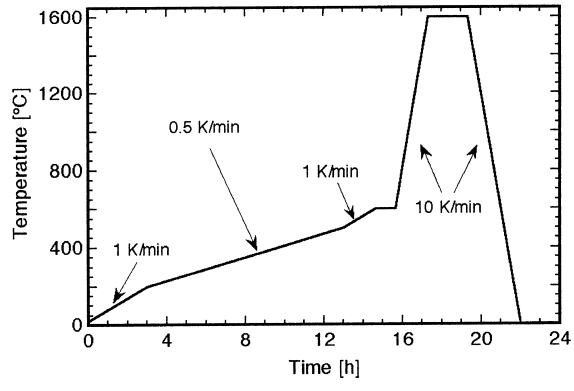

Fig. 4. Firing scheme of the laminates.

Instruments was used with a cone and plate geometry in oscillation mode at a frequency of 1 Hz.

To observe the polymeric reactions occurring during heat treatment, the double-sided adhesive tape was heated under an optical microscope (Orthoplan-Pol from Leitz Wetzlar). For that purpose a strip of the tape was glued between two glass plates and continuously heated at a rate of 5 K min^{-1} from room temperature to 340°C.

The polymer migration in the laminates during the burn-out procedure was also studied. The combination of Tape B with the double-sided adhesive tape was chosen. At 250°C and every 50 K up to 500°C, laminates were removed from the kiln, and the annealed specimens were broken and analysed using electron and optical microscopes.

To obtain a picture of the green tapes pore structure in relation to the powder skeleton, both tapes were sintered following the firing scheme in Fig. 4 to the onset of neck formation at 1050°C, which was determined by dilatometry. The pore size distribution was measured by the mercury intrusion technique, using a Porosimeter 2000 of Carlo Erba Instruments.

3 Results and Discussion

3.1 Quality of the laminates

The lamination experiments led to different qualities of junction for both green tapes. No defect free laminate of Tape A was obtained with the double-sided adhesive tape. A polished cross section of such a specimen is shown in Fig. 5(a). The remaining interfacial layers between the former green tapes are clearly detectable. At higher magnifications, these lines were identified as regions of higher porosity.

In contrast, the lamination of Tape B resulted in a homogeneous body without any zones of distortion. A representative laminate is shown in Fig. 5(b). After sintering the three layer laminate shows no defects.

For all combinations of green tape and gluing material, no dependency on the applied pressure during the lamination process was detectable. The different pressures of 2·5 and 5 MPa produced no changes in the results of the lamination experiments. Even a slight pressure produced by hand was sufficient for successful lamination.

This pressure independence is consistent with the fact that in all cases additional organic material is inserted between the ceramic layers: an 'interpenetration' of the particles does not occur during the lamination process. Moreover this leads to the assumption that the polymeric reactions occurring during heat treatment play an important role in the joining of the layers. Since the quality of the laminates was dependent on the green tape used, a key role can also be assigned to the green tapes microstructure. To study this further, the dependence of the polymer behaviour on temperature was investigated and the green tapes microstructures were analysed.

3.2 Thermal behaviour of the polymers

The double-sided adhesive tape, as shown in Fig. 3, basically consists of an approximately 12 μm thick backing of PET and an acrylate on each side as glue. The total thickness amounts to 48 μm. Observation under the optical microscope during heating revealed that the two materials behave differently. Figure 6 shows three pictures from a series of photographs taken during the experiment.

Figure 6(a) shows the initial condition at 25°C. Small air bubbles are trapped between the glass plate and the acrylate glue. As shown in Fig. 6(b), the polyacrylate starts to melt around 162°C, causing the air bubbles to enlarge due to expansion of the air. The expansion stops at 239°C, due to cross-linking of the acrylate layers. At 245°C, the polyester film between the immobile acrylate layers forms a low-viscosity melt. Figure 6(c) shows the condition at 260°C. The air bubbles are trapped in the acrylate, which is now cross-linked. The PET melt flows freely between the cross-linked adhesive

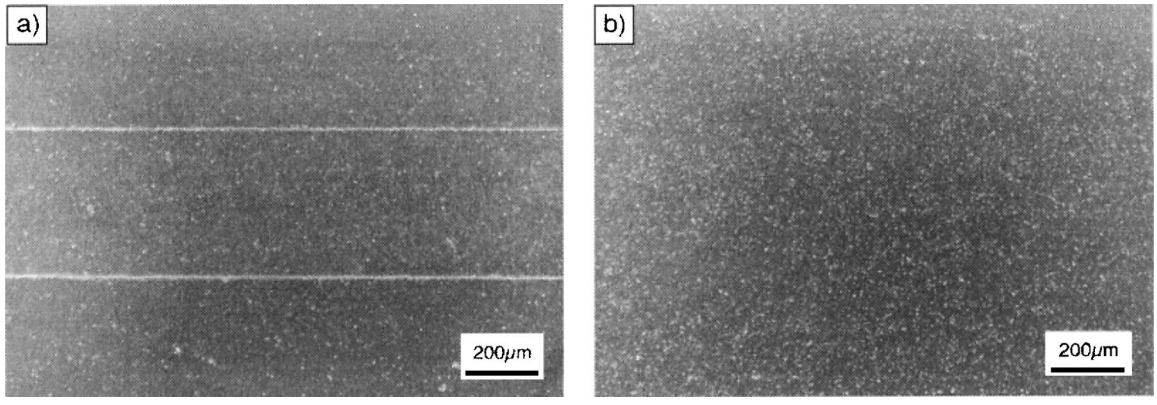

Fig. 5. (a) SEM image of the sintered laminate of Tape A, (b) SEM image of the sintered laminate of Tape B.

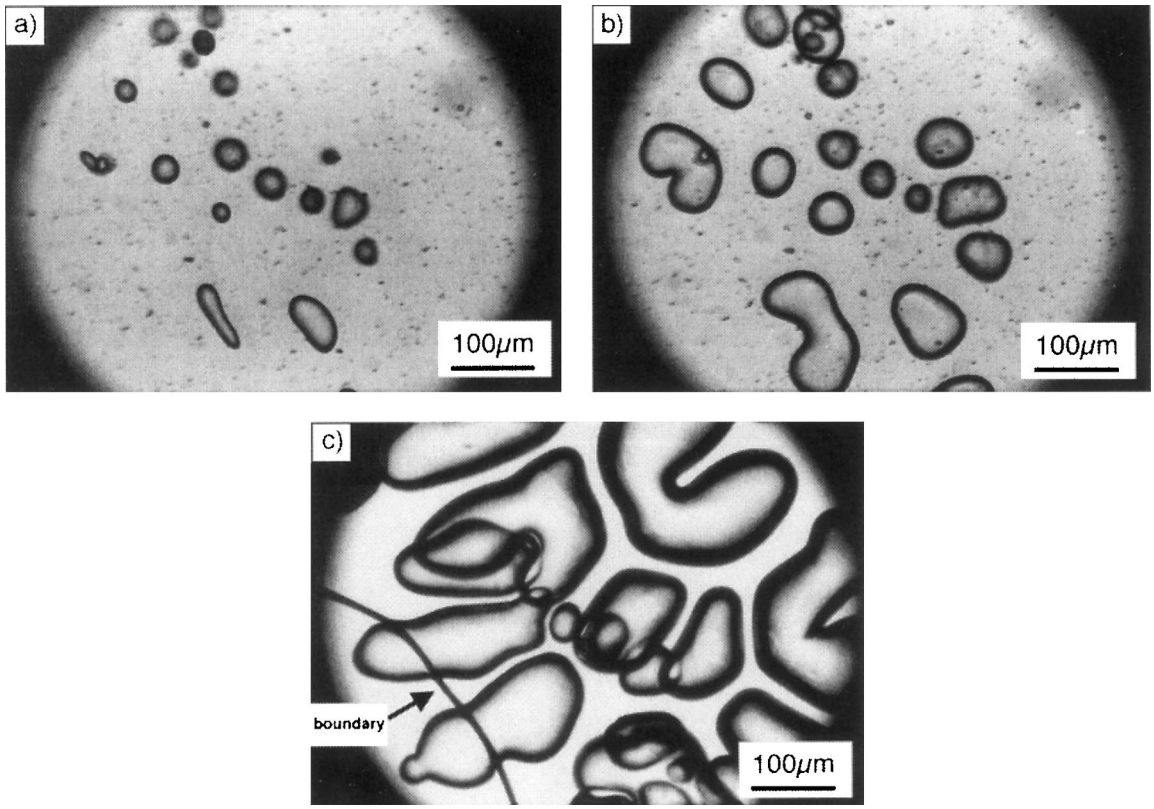

Fig. 6. Optical micrograph of the double-sided adhesive tape taken at (a) 25°C, (b) 162°C and (c) 260°C.

layers. A boundary between the low-viscosity melt and the outer atmosphere is visible.

This melting at a relatively high temperature is an outstanding property of the PET in comparison to the other organic materials used in the double-sided adhesive tape and the green tapes. Viscosity measurements of the PET and the binder system underline this effect (Fig. 7). Obviously the melting and the decrease in viscosity of the binder system take place in the temperature regime between 50°C and 150°C. In contrast, the PET starts melting at around 250°C with a relatively low viscosity. At around 283°C the curve bends, indicating the onset of degradation due to breaking of the molecular chains.

In the calorimetric and gravimetric analysis of the organic compounds, the differences were less pronounced. The TGA experiments on the PET and the acrylate showed almost the same temperature dependence, as can be seen in the TGA curves in Fig. 8. Only above 380°C did the mass loss of the acrylate differ considerably from that of the PET. Here the polyester experienced a greater mass loss. The binder system starts to decompose at significantly lower temperatures, but over a broad temperature range.

The DSC plots in Fig. 9 reveal that in every case, the main reaction enthalpies take place around 450°C. The acrylate and the binder system show similar behaviour with reaction enthalpies in the same range. For the binder system there are hardly any reactions detectable up to 410°C. The exothermic peak is relatively broad. This is typical for a binder system since such a behaviour decreases

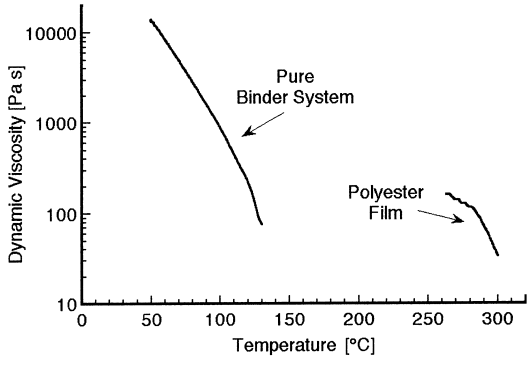

Fig. 7. Results of the dynamic viscosity measurements.

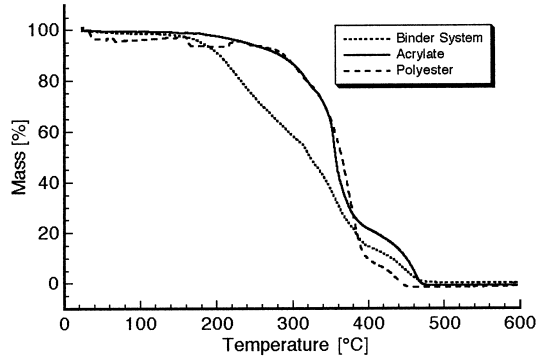

Fig. 8. TGA results for the polymers. The disturbance *t* in the curve of the PET in the beginning is caused by the low total weight of the sample.

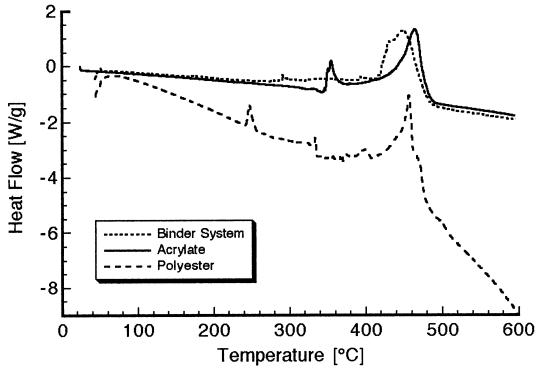

Fig. 9. DSC curves of the PET, the acrylate, and the binder system.

the evolution of crack gases and therefore reduces the sources of defects. A comparison of the adhesive tape materials illustrates their different natures. The reactions corresponding to PET removal are more endothermic than the ones of the acrylate adhesive, consistent with the different decomposition mechanisms. In the polyester, the molecular chains of the formed melt are broken into smaller units which evaporate from the liquid. In the beginning the acrylate also starts melting, but in contrast to the PET it starts to form a rigid network and react with the gaseous atmosphere; the immobile network leaves cracks and voids.[11] Since evaporation is an endothermic process, more energy is needed to remove the PET.

3.3 Microstructure of the ceramic tape

The porosity measurements of the powder skeletons of both tapes are shown in Fig. 10. Obviously the pore structures differ considerably. In the case of Tape A, the pore size distribution is narrower, with a mean pore size of 0·14 μm, while Tape B shows a broader distribution with a mean pore size of 0·60 μm.

3.4 Kinetics during binder burn-out

From the results it can be stated that capillary forces are present, because a porous body is in contact

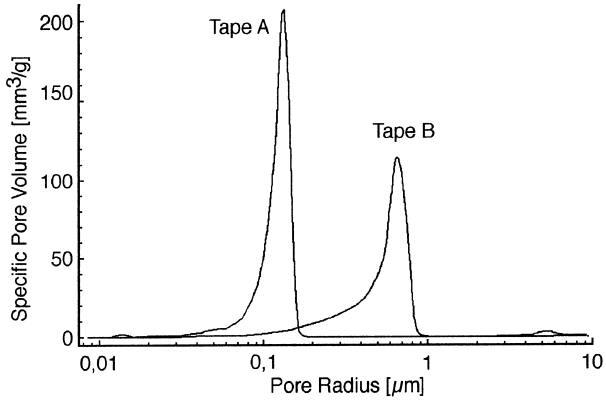

Fig. 10. Pore size distribution of both tapes after sintering at 1050°C.

with a liquid polymer melt which develops during binder burn-out. These capillary forces are responsible for the bonding of the ceramic layers during the firing process.

From that point of view the results of the TGA measurements seem to be contradictory to the good lamination results. According to Fig. 8 the mass losses of the PET and the acrylate take place in the same temperature range. Therefore the acrylate adhesive should function as a barrier for the polyester. The DSC measurements of Fig. 9 and the knowledge of the decomposition mechanisms can explain this discrepancy.

The decomposition mechanisms of the acrylate and the PET are different. Since the evaporation of the PET is more energy-consuming than the degradation of the acrylate, the adhesive is removed earlier than the polyester. Furthermore the acrylate stays in contact with the ceramic particles. In general, polymers in contact with ceramic powders decompose earlier due to the reduction of the activation energies.[12–14] For a PVB system with alumina powders Masia *et al.*[15] reported a shift of the TGA curve of about 100°C toward lower temperatures. Since the thermal conductivity of polymers is relatively low, the acrylate layers also function as thermal insulators. Therefore the PET lasts longer in the laminate than the acrylate.

The analysis of the laminates removed during the burn-out cycle supports this hypothesis. As shown in Fig. 11(a), at 350°C the remaining polymer phase is roughly 15 μm thick. This is close to the thickness of the PET film in the untreated double-sided adhesive tape. This indicates that almost all the acrylate has been removed, while the loss of the polyester is relatively small. At 400°C the polymer layer has been reduced to 5·4 μm, as Fig. 11(b) shows. This decrease in thickness during a temperature increase of 50°C can be attributed to flow of the polymer through the pores and evaporation at the increasing contact area of polymer and air.

In the literature, for binder systems such as PVB, the removal is attributed to the transport of the viscous binder phase.[16,17] The binder is transported through the smallest pores to the binder/air interface, where it evaporates and reacts with the kiln atmosphere.[11,18] The suction of the binder into the smallest pores creates a continuous pore channel system during the binder removal.[18]

This reflection helps to explain the joining mechanism. The driving force for the joining of the tapes is the capillary pressure that exists during the burn-out process. If most of the binder that fixes the ceramic particles in the green tape is removed, the PET-polymer melt between the ceramic layers is dragged through the open channel system by capillary forces. As is the case during the binder

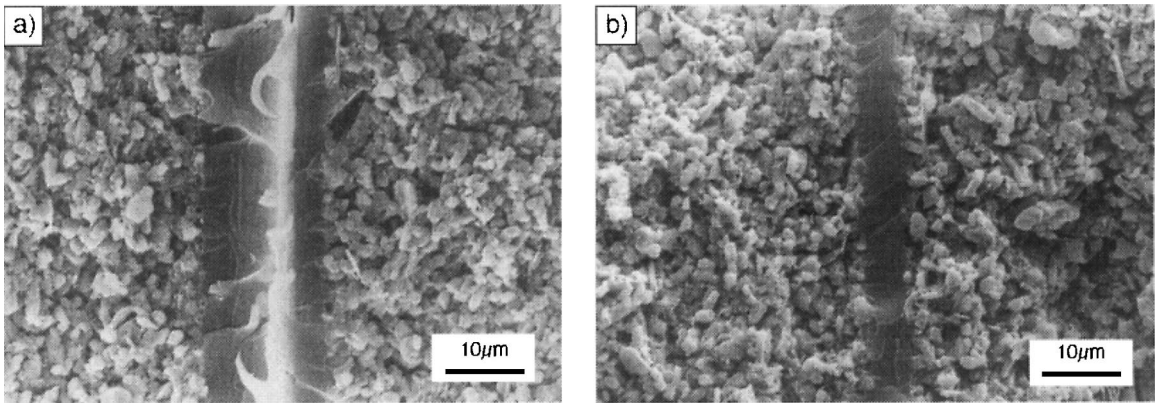

Fig. 11. Fracture surfaces of laminates removed at different temperatures from the kiln: (a) at 350°C, a polymer layer of 14·7 μm is left: (b) at 400°C, the layer thickness is reduced to 5·4 μm.

decomposition, the transport of the melt takes place through the smallest pores. The removal of the melt creates a drag on the ceramic layers and causes them to approach each other. Figure 12 shows a model of this process. The viscosity of the melt drops with increasing temperature, increasing the flow of the melt. Since the ceramic particles are no longer embedded in the binder matrix, the particles at the edges can rearrange and move so that the ceramic layers interpenetrate each other due to the capillary forces. From that point of view the proposed model of Hellebrand[7] is still valid; however, the necessary pressure for rearrangement of the particles is not created by externally applied forces during the lamination process but from internal capillary pressure during binder burn-out.

$$\Delta p = \frac{2\gamma_{LV}\cos\theta}{r_p} \tag{1}$$

$$\bar{v} = \frac{\Delta p r_p^2}{8L\eta} \tag{2}$$

$$\bar{v} = \frac{\gamma_{LV}\cos\theta}{\eta}\,\frac{r_p}{4L} \tag{3}$$

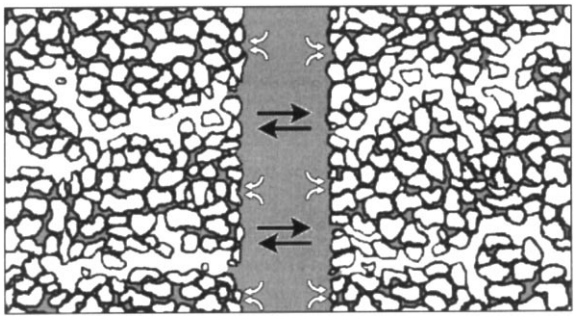

Fig. 12. A model of the melt flow through the smallest pores causing the ceramic layers to approach each other. The white arrows indicate the flux of the polymer melt, while the black arrows represent the approach of the ceramic layers towards each other.

where

Δp = capillary pressure;
γ_{LV} = surface tension;
θ = wetting angle;
r_p = pore diameter;
$\bar{v}$ = average laminar flow velocity;
L = length of cylindrical pore;
η = viscosity of the melt.

The forces acting in the process as well as the interaction of the polymer melt with the microstructure of the ceramic tapes are described by the equations above. The capillary pressure in the presence of a liquid is given by the Laplace equation [see eqn (1)]. The average laminar flow velocity can be expressed by the Poiselle equation [see eqn (2)]. Both equations show the opposing effects the pore structure has on the polymer melts. According to eqn (1), a finer pore size leads to higher capillary forces. On the other hand, a finer particle size decreases the flow of the melt through the pores. Therefore a finer pore size is not necessarily beneficial to the whole process. Combining eqns (1) and (2) leads to eqn (3), the Hagen–Poiselle equation. The first term in the equation describes properties of the polymer melt, whereas the second term represents the characteristics of the pores in the tape.

The equations help to explain the different lamination results of the two green tapes. The PET melts at temperatures at which most of the binder has been removed or moved back into the smallest pores. Furthermore, the melts viscosity is relatively low. Therefore, the melt can flow even more freely [see eqn (3)]. In Tape B the pore size distribution is relatively broad. Its mean pore size ($d_{\text{pore},50}$ $\sim$0·6 μm) is relatively large compared to that of Tape A ($d_{\text{pore},50}\sim$0·14 μm). Even if residues of the binder block small pores in Tape B, there is sufficient free pore volume for the PET to drain away. The increased pore size enhances the flow of the

polymer melt [see eqns (2) and (3)]. At the end of this process the particles of the ceramic layers can interpenetrate each other. Since the particles and pores are relatively coarse, the bridging and interpenetration is facilitated. Remaining voids might also be removed during the melting of the glass phase at higher temperatures. A good laminate quality after sintering is obtained.

Obviously the bridging and interpenetration of the particles is not as effective for Tape A as for Tape B, as can be seen in Fig. 5(a) and (b). The line of pores remaining between the layers in the laminate of Tape A may be attributed to the microstructure of the ceramic tape. In Tape A, the free flow of the polymer melt is lower due to the smaller pore size [see eqns (2) and (3)], whereas the capillary forces are higher [see eqn (1)]. Residues of the binder that might be left in smaller pores might also hinder the melt flow since the pore size distribution of Tape A is relatively narrow. The kinetic process of the PET melt flow with respect to particle interpenetration seems to be to less effective although the particle size is smaller. The surface roughness of the moving carrier film, which is part of the tape casting apparatus, caused surface defects in Tape A. These cannot be bridged by the fine particles, thus leaving pores in the interface.

The fact that polymer melts are created in the green body during firing is common knowledge. Moreover this effect is exploited for the binder burn-out procedure since it ensures a homogeneous removal of binder and binder residues in the body, reducing the probability of flaw formation.[12] The new aspect of this study is that additional thermoplastic material is inserted into the green body. Although concentrated in a certain volume of the ceramic specimen the polymer acts as an aid for a manufacturing process: the joining of ceramics.

4 Conclusion

The experiments proved that lamination using adhesive materials is possible at room temperature with low pressures. The sticking properties of the adhesive play a minor role. They ensure the fixing of the green tapes for handling. A prerequisite for a successful lamination is the creation of a low-viscosity melt at relatively high temperatures. This is fulfilled by the double-sided adhesive tape. The drag of the melt through the pores causes the ceramic tapes to approach one another and form a junction. One prerequisite is the formation of a pore channel system with sufficient free volume for the flow of the polymer melt in the green tape during the binder burn-out. In addition, a sufficient grain size of the powder particles is needed to enable the green sheets to interpenetrate each other.

With this lamination technique the former problems of deformation during lamination can be overcome, which is important for the realisation of new applications for laminated complex 3D structures.

Acknowledgements

The authors would like to thank Dr. Ruska and Dr. Thimm from CeramTec AG, Dr. Storbeck from Beiersdorf AG and Dr. Kaschta from the Department of Materials Science, Polymer Materials at the University of Erlangen-Nuremberg for the helpful discussions. Special thanks to Dr. Kaschta for his support in the viscosity measurements.

References

1. Mistler, R. E., Shanefield, D. J. and Runk, R. B., Tape casting of ceramics. In *Ceramic Processing Before Firing*, eds. G. J. Onoda and L. L. Hench, John Wiley and Sons, New York, 1978, pp. 411–448.
2. Heinrich, J., Huber, J., Schelter, H., Ganz, R., Golly, R., Foerster, S. and Quell, P., Compact ceramic heat-exchangers: design, fabrication and testing. *Brit. Ceram. Trans. J.*, 1987, **86**(6), 178–182.
3. Minh, N. Q., Ceramic fuel cells. *J. Am. Ceram. Soc.*, 1988, **76**(3), 563–588.
4. Cawley, J. D., Heuer, A. H., Newmann, W. S. and Mathewson, B. B., Computer-aided manufacturing of laminated engineering materials. *Amer. Ceram. Soc. Bull.*, 1996, **75**(5), 75–79.
5. Mistler, R. E., Tape casting: the basic process for meeting the needs of the electronics industry. *Amer. Ceram. Soc. Bull.*, 1990, **69**, 1022–1026.
6. Reed, J. S., *Principles of Ceramics Processing*, 2nd Ed., John Wiley & Sons, New York, 1994.
7. Hellebrand, H., Tape casting. In *Materials Science and Technology*, Vol. 17A, *Processing of Ceramics, Part 1*, ed. R. J. Brook. VCH Verlagsgesellschaft, Weinheim, FRG 1996, pp 189–265.
8. Roosen, A., Basic requirements for tape casting of ceramic powders. In *Ceramic Transactions*, Vol. 1, *Part B, Ceramic Powder Science*. American Ceramic Society, Westerville, Ohio, 1988, pp 675–692.
9. Chartier, T., Streicher, E. and Boch, P., Phosphate esters as dispersants for the tape casting of alumina. *Amer. Ceram. Soc. Bull.*, 1987, **66**(11), 1653–1655.
10. WWW-page: http://www.tesa.de/g/gs/xgs.htm, Beiersdorf AG, Hamburg.
11. Lewis, J. A., Cima, M. J. and Rhine, W. E., Direct observation of preceramic and organic binder decomposition in 2-D model microstructures. *J. Am. Ceram. Soc.*, 1994, **77**(7), 1839–1845.
12. Ferrato, M., Chartier, T., Baumard, J. F. and Coudamy, G., Der Bindemittelabgang in keramischen Scherben. *CFI/Ber. DKG*, 1994, **73**(1–2), 8–12.
13. Yang, T. C., Chang, W. H. and Viswanath, D. S., Thermal degredation of poly(vinyl butyral) in alumina, mullite and sillica composites. *J. Thermal Anal.*, 1996, **47**, 697–713.
14. Wessley, E., Frey, T. and Roosen, A., Influence of different parameters on binder burn-out of ceramic green bodies. In *Euro Ceramics II*, ed. G. Ziegler and H.

Hausner, Deutsche Keramische Gesellschaft, Köln, 1993, pp. 435–439.
15. Masia, S., Calvert, P. D, Rhine, W. E. and Bowen, H. K., Effect of oxides on binder burn-out during ceramics processing. *J. Mat. Sci.*, 1989, **24**, 1907–1912.
16. Calvert, P. and Cima, M., Theoretical models for binder burn-out. *J. Am. Ceram. Soc.*, 1990, **73**(3), 575–579.
17. Cima, M. J., Dudziak, M. and Lewis, J. A., Observation of poly(vinyl butyral)-dibutyl phthalate binder capillary migration. *J. Am. Ceram. Soc.*, 1989, **72**(6), 1087–1090.
18. Cima, M. J., Lewis, J. A. and Devoe, A. D., Binder distribution in ceramic greenware during thermolysis. *J. Am. Ceram. Soc.*, 1989, **72**(7), 1192–1199.